Hydrogen isotopes in high ³He/⁴He submarine basalts: Primordial vs. recycled water 1 2 and the veil of mantle enrichment 3 Matthew W. Loewen*^{1,3}, David W. Graham², Ilya N. Bindeman³, John E. Lupton⁴, 4 5 Michael O. Garcia⁵ 6 7 *Corresponding author: mloewen@usgs.gov 8 1. Alaska Volcano Observatory, U.S. Geological Survey, Anchorage, AK 99508 9 2. College of Earth, Ocean, and Atmospheric Sciences, Oregon State University, 10 Corvallis, OR 97331 11 3. Department of Earth Sciences, University of Oregon, Eugene, OR 97403 12 4. NOAA Pacific Marine Environmental Laboratory, Newport, OR 97365 13 5. Department of Geology & Geophysics, SOEST, University of Hawaii, Honolulu, HI 14 96822 15 16 **Abstract** 17 The hydrogen isotope value (δD) of water indigenous to the mantle is masked by the early degassing and recycling of surface water through Earth's history. High ³He/⁴He 18 19 ratios in some ocean island basalts, however, provide a clear geochemical signature of 20 deep, primordial mantle that has been isolated within the Earth's interior from melting, 21 degassing, and convective mixing with the upper mantle. Hydrogen isotopes were measured in high ³He/⁴He submarine basalt glasses from the Southeast Indian Ridge 22 (SEIR) at the Amsterdam-St. Paul (ASP) Plateau ($\delta D = -51$ to -90%, $^{3}He/^{4}He = 7.6$ to 14.1 23

 R_A) and in submarine glasses from Loihi Seamount south of the island of Hawaii ($\delta D = -$ 70 to -90%, ${}^{3}\text{He}/{}^{4}\text{He} = 22.5$ to 27.8 R_A). These results highlight two contrasting patterns of δD for high ${}^{3}\text{He}/{}^{4}\text{He}$ lavas: one trend toward high δD of approximately -50%, and another converging at $\delta D = -75\%$. These same patterns are evident in a global compilation of previously reported δD and ${}^{3}He/{}^{4}He$ results. We suggest that the high δD values result from water recycled during subduction that is carried into the source region of mantle plumes at the core-mantle boundary where it is mixed with primordial mantle, resulting in high δD and moderately high ${}^{3}\text{He}/{}^{4}\text{He}$. Conversely, lower δD values of -75%, in basalts from Loihi Seamount and also trace element depleted mid-ocean ridge basalts, imply a primordial Earth hydrogen isotopic value of -75‰ or lower. δD values down to -100% also occur in the most trace element-depleted mid-ocean ridge basalts, typically in association with 87 Sr/ 86 Sr ratios near 0.703. These lower δD values may be a result of multi-stage melting history of the upper mantle where minor D/H fractionation could be associated with hydrogen retention in nominally anhydrous residual minerals. Collectively, the predominance of δD around -75% in the majority of mid-ocean ridge basalts and in high ³He/⁴He Loihi basalts is consistent with an origin of water on Earth that was dominated by accretion of chondritic material. **Keywords:** hydrogen isotopes; water; helium isotopes; primordial mantle; Loihi; Amsterdam-St. Paul

24

25

26

27

28

29

30

31

32

33

34

35

36

37

38

39

40

41

42

43

44

45

47

48

49

50

51

52

53

54

55

56

57

58

59

60

61

62

63

64

65

66

67

68

69

1. Introduction

Water on the Earth's surface is essential for the development of life. In the mantle it contributes to partial melting and rheological behavior during solid state convection (e.g., McGovern and Schubert, 1989; Hirschman, 2006). Despite this first-order importance for planetary evolution, a basic question remains regarding how much water in mantlederived magmas is juvenile, i.e., primordial water that has never been present at Earth's surface (representing original accreted planetary water), versus water from recycling by subduction throughout Earth's history (e.g., Lécuyer et al., 1998; Hirschmann, 2006; Marty, 2012; Parai and Mukhopadhyay, 2012; Peslier et al., 2017). This question may be addressed by coupling measurements in mantle-derived materials of water and its isotopic composition with other indicators of mantle provenance. The deuterium/hydrogen ratio is the most diagnostic, and is expressed in delta notation relative to standard mean ocean water as $\delta D = \{(D/H)_{sample}/(D/H)_{SMOW} - 1\} \times 10^3$. High ³He/⁴He ratios associated with ocean island basalt (OIB) volcanism track the presence of primitive mantle that has been isolated from melting and degassing since the earliest stages of Earth history (e.g., Allègre et al., 1983; Mukhopadhyay, 2012). Only a few studies have directly compared δD measurements with ³He/⁴He, despite the fact that both hydrogen and helium should be incompatible during mantle melting (Aubuad et al., 2004; Graham et al., 2016), therefore making high ³He/⁴He samples a prime target for understanding primordial hydrogen isotopic values (Craig and Lupton, 1976; Rison and

Craig, 1983; Poreda et al., 1986). These earlier studies, however, found that a high ³He/⁴He signature is variably coupled with tracers of mantle enrichment, such as isotopes of Sr-Nd-Pb, that represent the time integrated history of mantle melting and subduction recycling. These co-variations suggest that recycled and primordial material can be admixed in the mantle (e.g., Kurz et al., 1982; Hanan and Graham, 1996), and this has prevented an unambiguous characterization of primordial hydrogen isotope values. The early study by Poreda et al. (1986) of basalts from the Reykjanes, Kolbeinsey, and Mohns Ridges around Iceland showed that δD was best correlated with trace element indicators of mantle enrichment such as La/Sm, and also with total water concentrations. Trace element ratios and water concentrations can reflect both the character of the mantle source and/or the degree of partial melting. The results for ${}^{3}\text{He}/{}^{4}\text{He}$ and δD showed diverging trends, to both high and low δD (-50% and -90%) in the highest ${}^{3}\text{He}/{}^{4}\text{He}$ samples from the Reykjanes Ridge. Ultimately, Poreda et al. (1986) could not determine whether the high δD values in high ${}^{3}\text{He}/{}^{4}\text{He}$ basalts indicated a stronger component of primordial water vs. water derived from recycled lithosphere/crust. A stronger relationship of high δD and high $^{3}He/^{4}He$ is present for basalts from the Easter Island hotspot region of the East Pacific Rise (data from Poreda et al., 1993; Kingsley et al., 2002). However, those results also do not resolve if the δD values were primarily influenced by recycled or primordial water, or both. The recent comprehensive study of water and D/H in global mid-ocean ridge basalts (MORB) by Dixon et al. (2017) indicates the presence of a diversity of enriched

70

71

72

73

74

75

76

77

78

79

80

81

82

83

84

85

86

87

88

89

90

91

components. Dixon et al. (2017) proposed that many subducting slabs undergo a primary phase of dehydration, followed by a secondary phase of rehydration due to the release of water from alteration minerals within cooler parts of the slabs at greater depths. Slab temperature is a key variable in the Dixon et al. (2017) model, and it largely dictates the degree of coupling between H₂O and lithophile element tracers. According to this model, the entire global range of mantle δD is a result of differences in the evolution of hot vs. cold slabs during subduction. Dixon et al. (2017) concluded that interaction with primordial material might occur during slab recycling to the deep mantle, but they did not investigate co-variations between δD and ³He/⁴He. Defining Earth's primordial δD has been elusive, with values proposed as extreme as δD =-218% (Hallis et al., 2015) to values of -60 to -80% that are more typical of MORB (Lécuyer et al., 1998). The more traditional MORB-like value for primordial δD in Earth matches average meteoritic δD values and has been taken as support for a chondritic origin of Earth's water (Marty and Yokochi, 2006). In contrast, the much lower δD value suggested from melt inclusion studies of high ³He/⁴He basalts from Baffin Island (Hallis et al., 2015) may point to trapped water from solar nebula gas during accretion. However, the accurate determination of δD values and water concentrations in melt inclusions are difficult and can be problematic (e.g., Hauri, 2002; Portnyagin et al., 2008; Gaetani et al., 2012), and questions remain about how to best interpret very low δD values for Baffin melt inclusions (Michael, 2017; Gatti et al., 2018). An improved characterization of δD variations in high ${}^{3}\text{He}/{}^{4}\text{He}$ submarine glasses is needed to understand the primordial δD composition of the Earth.

93

94

95

96

97

98

99

100

101

102

103

104

105

106

107

108

109

110

111

112

113

114

Advances in continuous flow mass spectrometry (Sharp et al., 2001; Bindeman et al., 2012; Martin et al., 2017) allow analyzing D/H ratios and water concentrations on milligram quantities of water-poor glass, which is 100 times less material than by conventional methods. This permits analysis of the purest glass concentrate. In this study we utilized these methods to analyze submarine glasses from localities with high ${}^{3}\text{He}/{}^{4}\text{He}$ basalt: the Southeast Indian Ridge (SEIR) in the vicinity of the Amsterdam-St. Paul (ASP) Plateau and Loihi Seamount south of the island of Hawaii (Fig. 1). Both localities represent the surface manifestation of a mantle plume and have ³He/⁴He that extends well above the values typically found in upper mantle-derived basalts; ³He/⁴He in some Loihi Seamount lavas are among the highest measured at ocean islands. These localities are also well characterized in their trace element and Sr-Nd-Pb isotopic compositions, but they have not been investigated in detail for D/H ratios. These new results are synthesized with previous analyses of δD and ${}^{3}He/{}^{4}He$ in oceanic basalts worldwide (**Fig.** 1; Dixon et al., 2017). Collectively these data sets provide a more robust framework to evaluate the hydrogen isotopic composition of the deep mantle and the potential contributions of primordial water and recycled water to ocean ridge and mantle plume basalts.

134

135

136

137

138

116

117

118

119

120

121

122

123

124

125

126

127

128

129

130

131

132

133

2. Samples and methods

2.1. Sample selection

The SEIR crosses the ASP Plateau in the southern Indian Ocean. The plateau contains numerous seamounts and the two islands of Amsterdam and St. Paul, which lie

approximately 60 and 100 km, respectively, from the nearby spreading ridge. Submarine basalts from the SEIR atop the plateau, and from the areas to the northwest and the southeast of the plateau, have been recovered at roughly 10-15 km spacing. These basalts are well characterized for major elements and He-Sr-Nd-Pb isotopes (Douglas-Priebe, 1998; Graham et al., 1999; Johnson et al., 2000; Nicolaysen et al., 2007). Notably for our study, ³He/⁴He values are elevated, up to 14 R_A (where R_A is the atmospheric ³He/⁴He ratio), on the ASP plateau and along the spreading the ridge segment (H) immediately to its northwest. Submarine glasses were analyzed for δD and H_2O from 18 dredge and wax core locations along the SEIR, collected by the R/V Melville during the Boomerang 06 expedition. Samples selected for this study contain 0.1 to 1 wt.% water and were all collected at water depths greater than 1500 m (>15 MPa). At these depths, water concentrations up to 1.25 wt.% should remain saturated in a basaltic melt (Newman and Lowenstern, 2002). Trace element data for these samples have been obtained by Laser Ablation-Inductively Coupled Plasma-Mass Spectrometry (LA-ICP-MS) using methods similar to those described in Michael and Graham (2015) and Loewen and Kent (2012) and are reported in Table S1. Loihi Seamount is the youngest expression of active volcanism associated with the Hawaiian hotspot (Moore et al., 1982). It lies about 35 km south of Hawaii and is constructed on the submarine flanks of Mauna Loa and Kīlauea. Loihi lavas show limited Sr-Nd-Pb isotopic variability with no correlation with degree of silica saturation or age;

139

140

141

142

143

144

145

146

147

148

149

150

151

152

153

154

155

156

157

158

159

160

thus the range in rock compositions is thought to be derived by variable degree of melting of a common mantle source (Garcia et al., 1989, 1993, 1998). 3 He/ 4 He values of Loihi basalts range to values >30 R_A (Kurz et al., 1983; Rison and Craig, 1983).

Thirteen submarine basalt glasses were analyzed from Loihi Seamount. These samples were collected in 1983 by dredges from the R/V *Kana Keoki*, in 1987 by the *Alvin* submersible during dives 1801-1804, and in 1996 by the *Pisces V* submersible during dive 286 following the 1996 Loihi summit eruption. Major, trace, volatile, and isotopic data for these samples are reported in Garcia et al. (1989, 1993, 1998), and Pietruszka et al. (2011). Rock types analyzed include tholeitic, transitional, and alkali basalts. The Loihi samples were erupted at shallower depths (1000-1350 m) than the analyzed SEIR glasses, and hence we critically assess the potential degassing effects for that sample suite.

2.2. Hydrogen isotope analyses

Determinations of δD and total water concentrations were made by a Thermal Conversion Elemental Analyzer (TC/EA) coupled to a MAT 253 10 kV gas source isotope ratio mass spectrometer (IRMS) at the University of Oregon (Bindeman et al, 2012; Martin et al. 2017). Clean, unaltered glass was crushed and sieved to the 250-50 μ m size fraction and visually inspected to ensure purity of the glass separate, 5-10 mg wrapped into silver capsules, heated in a ~150 °C vacuum overnight to remove adsorbed water, and loaded into a He-purged autosampler. Samples were run in 2-6 replicates. All individual sample analyses are reported in the **Table S2**. Values of δD used for plotting,

and for comparison between samples, are the medians of these replicate analyses. The median limits the influence of an occasional disparate measurement more effectively than the mean. Multiple standards were analyzed concurrently with the unknown glasses during each analytical session, including direct standard waters welded in silver cups: VSMOW (0%), W62001 (-41.5%), and Lake Louise (-150.2%) produced by the U.S. Geological Survey (Qi et al., 2010). Solid standards included in-house micas: NBS30 (-50.0%), RUH2 (-81.4%), BUD (-144.7%), as well as recently calibrated mica standards USGS57 (-91‰), and USGS58 (-28‰) (Qi et al., 2017). We note that our nominal value of NBS30 is 16% higher than the -65.7% reference value used in the majority of historical studies (see Martin et al. 2017 for discussion). Our offset is a result of direct measurement of NBS30 relative to water standards in our TC/EA system and a now recognized offset between TC/EA and conventional δD determinations (Qi et al., 2014; 2017); this offset is likely a result of heterogeneity in NBS30 splits related to grain size variations (see Martin et al., 2017 and Qi et al., 2017 for a detailed discussion). We caution against directly comparing these results to studies that rely on NBS30 as a reference standard without correcting for heterogeneity of any particular split of standard. For analytical sessions utilized in this dataset, the 2σ reproducibility for NBS30 =5.5% $(n = 19 \text{ excluding a single } > 3\sigma \text{ outlier})$, RUH2 = 3.0% (n = 16), and BUD = 6.0% (n = 19). The average range of replicate analyses for individual samples is 5‰, although some

185

186

187

188

189

190

191

192

193

194

195

196

197

198

199

200

201

202

203

204

205

206

207

Loihi samples had a range of values in replicate analyses of up to 20%. We suggest this

larger range is indicative of sample heterogeneity due to hydrogen isotope fractionation during loss of small amounts of H_2O by degassing (see section 3.2 for more discussion). Median values were used for each sample to reduce the effects of sample heterogeneity. We focus on comparing our new δD data to previously published TC/EA data, due to systematic offsets that may exist between TC/EA and other methods. Dixon et al. (2017) described a ~10% systematic offset between 6 samples measured by both TC/EA and conventional stepped-heating manometry. Clog et al. (2012) also observed similar offsets between different conventional techniques. It is currently unclear which method provides a more accurate measurement of δD , and there are insufficient replicate data to provide an accurate interlaboratory correction. Total water concentrations were determined by peak integration during the TC/EA analyses, using a nominal 3.5 wt.% in the NBS30 biotite mica standard. Rapid thermal pyrolysis of hydrous glasses by TC/EA at 1450°C releases 100% of water in glass. This is established by comparison to independently determined (by FTIR or manometry) water concentrations for the same aliquots of basalt glasses in a wide range of H₂O from 0.1 to 1.2 wt.%, including water-poor glasses having <0.5 wt.% H₂O (Bindeman et al., 2012; Martin et al., 2017; Dixon et al., 2017). 2.3. Helium isotope analyses Helium isotope results for the SEIR sample suite were reported previously (Graham et al., 1999; Nicolaysen et al., 2007). **Table S3** provides results for 11 new He analyses

208

209

210

211

212

213

214

215

216

217

218

219

220

221

222

223

224

225

226

227

228

229

from Loihi Seamount along with 2 previously reported values (samples 286-1 and 286-5) from Garcia et al. (1998). All basalt glasses from Loihi were analyzed at NOAA/PMEL in Newport, Oregon, following methods outlined in Graham et al. (1999). Samples were lightly crushed and 1-5 mm-sized chunks of fresh glass free of alteration were selected using a binocular microscope. The selected glass was cleaned ultrasonically in deionized water and acetone and air dried. Sample weights ranged between 280 and 475 mg. The selected glass samples were crushed on-line to release the gas trapped in vesicles for He isotope analysis. Sample powders retrieved from the crushers were transferred to a high temperature vacuum furnace to also measure [He] and ${}^{3}\text{He}/{}^{4}\text{He}$ dissolved in the glass. The crushed powders were transferred to Al-foil boats, dropped into the furnace crucible and melted at 1400°C. Processing line blanks were analyzed before each sample and ranged from ~2 to 4 x10⁻¹⁰ cm³ STP ⁴He. The He concentration and isotope value of samples were calibrated against aliquots of known size of marine air collected in Newport. Aliquots of a geothermal gas secondary standard, collected from Yellowstone Park (MM = Murdering Mudpots, having ${}^{3}\text{He}/{}^{4}\text{He} = 16.5 \text{ R}_{A}$), were also analyzed routinely to correct for small (<3%) mass discrimination effects related to variations in gas pressure in the mass spectrometer.

248

249

250

251

252

253

231

232

233

234

235

236

237

238

239

240

241

242

243

244

245

246

247

3. Results and Discussion

3.1. Southeast Indian Ridge

δD varies along the SEIR between -90‰ and -51‰, covering much of the range of δD reported globally for oceanic basalts (Kyser and O'Neil, 1984; Poreda et al., 1986; Kingsley et al., 2002; Dixon et al., 2017). Higher δD values are generally associated with

geochemically enriched samples in the ASP Plateau region (Fig. 2). The strongest covariations involving δD are with incompatible species (e.g., water, K_2O , La), and with ratios of highly incompatible/moderately incompatible elements (e.g., La/Sm, K/Ti; see Fig. S1). These ratios and concentrations can reflect either enriched incompatible element concentrations in the source region or low degrees of partial melting, or both. The highest δD values (DR64-2, WC37 and WC47) tend to be associated with the radiogenic ²⁰⁶Pb/²⁰⁴Pb signature of the ASP mantle plume and are found throughout the plume influenced region (on ridge segments I, J, and H; Fig. 2). This plume Pb isotopic composition is identical to the common (C)-type composition described by Hanan and Graham (1996) in their treatment of global MORB and OIB data sets. The most enriched SEIR lavas having this signature are erupted along segment H, located immediately northwest of the ASP Plateau (Fig. 1). Segment H is also characterized by very large He-Pb-Sr-Nd isotopic diversity (Graham et al., 1999; Nicolaysen et al., 2007). The new results presented here show that this diversity also characterizes hydrogen isotopes. For example, there is a systematic decrease in δD of segment H lavas, from enriched (e.g., high La/Sm; WC47, $\delta D = -53$ ‰) to depleted basalts (e.g., low La/Sm; DR73-6, $\delta D = -53$ ‰) 79‰). Some lavas atop the ASP Plateau (on segments I and J) have a distinct isotope composition characterized by markedly higher ⁸⁷Sr/⁸⁶Sr and ²⁰⁸Pb/²⁰⁶Pb (**Figs. S1, S2**), referred to as Dupal-type (Hart, 1984), possibly a reflection of recycled lower continental crust or lithosphere (e.g., White, 2015). These Dupal-type basalts do not all seem to exhibit high δD values (e.g., DR59-1, δD =-76%; **Fig. 2**).

254

255

256

257

258

259

260

261

262

263

264

265

266

267

268

269

270

271

272

273

274

The high δD values in ASP basalts are a signature of their mantle source, and do not result from secondary processes such as (1) shallow degassing, (2) seawater contamination, or (3) magma evolution/crystal fractionation as discussed below. Our observations exclude shallow degassing and any associated H₂O loss as a significant process in producing the observed δD variations. Degassing will lower the δD value of a residual melt, as D will be concentrated in the vapor phase molecular water (e.g., Hauri, 2002; De Hoog et al., 2009). In our analyzed basalts, samples with the highest water concentrations, and therefore having the potential for larger amounts of water loss accompanying the degassing of CO_2 -saturated melts (Fig. 3A), actually have the highest δD values. This is the opposite to the expectation that residual water in partially degassed melts will have lower δD (Fig. 3B). Seawater contamination can be examined in submarine glasses with measurements of Cl (**Fig. 4**). Two samples from segment I atop the ASP Plateau have elevated [Cl] and excess Cl (Cl that results from seawater or brine assimilation, as opposed to mantle melting or crystal fractionation processes. Excess Cl is computed from the relation between Cl/K and K/Ti; see Michael and Cornell, 1998). Segment H basalts that do not have elevated Cl contents or Cl/K ratios, however, have similar δD values. Also, MORB glasses having high Cl or Cl/K do not typically show anomalously high δD as might be expected from seawater assimilation (Figs. 4 and S1; Kingsley et al., 2002; Clog et al., 2013). This observation suggests that the process responsible for the elevated Cl in most ocean ridge basalts may be assimilation of halite that has minimal water content and high

276

277

278

279

280

281

282

283

284

285

286

287

288

289

290

291

292

293

294

295

296

297

Cl (e.g., Michael and Cornell, 1998; Kent et al., 1999; Pietruszka et al., 2011), and thus has little effect on δD values.

Crystal fractionation of non-hydrous minerals should not fractionate hydrogen isotopes and therefore crystal fractionation during magma evolution in the crust cannot be responsible for the observed δD variations in the SEIR basalts. Although some fractionated low MgO (<7.5 wt.%) basalts have relatively high δD values, elevated δD values are also found in high MgO basalts from segment H (**Fig. 2**), supporting this contention.

Finally, we also note that the lowest δD value in the SEIR basalt suite occurs in the most trace element depleted MORB glass (DR75-1, δD =-90‰) that was collected from a short relay zone within the Zeewolf Transform between segments H and G.

3.2. Loihi Seamount

The Loihi glass samples show a narrow range of ${}^{3}\text{He}/{}^{4}\text{He}$ for the gas trapped in vesicles (21.4-27.8 R_A) that is released by crushing in vacuum (one sample, ALV1803-14, is an exception: it has of a very low [He] <2x10⁻⁹ cm³ STP/g and ${}^{3}\text{He}/{}^{4}\text{He}$ <14 R_A). The range of ${}^{3}\text{He}/{}^{4}\text{He}$ in samples analyzed here overlaps previously reported values from Loihi (e.g., Kurz et al., 1983; Rison and Craig, 1983; Honda et al., 1993). These values are among the highest measured ${}^{3}\text{He}/{}^{4}\text{He}$ ratios in submarine basalt glasses from plumederived ocean island localities. Melting of the powders retrieved after the crushing analyses revealed a larger range of ${}^{3}\text{He}/{}^{4}\text{He}$ (10.3-26.3 R_A) in the glass that extends to

lower values than observed in the vesicles. Three samples show a significant amount He isotope disequilibrium between vesicles and glass (1802-4B, 1803-14, 1804-19); these samples have the lowest amount of He dissolved in the glass phase. This suggests that at these low dissolved He concentrations we can detect ingrowth of post-eruptive radiogenic ⁴He (Graham et al., 1987). We calculated ages of 2.0 to 7.3 kyrs for these three samples given their measured He isotope disequilibrium and reported U and Th concentrations (see Supplementary Material and Table S3 for further discussion). Other Loihi basalts have similar vesicle and melt ³He/⁴He, so estimates of their eruption ages are not possible from the He isotope disequilibrium method. The Loihi basalts are relatively evolved magmas (MgO =5-8 wt.%) and less compositionally diverse than the ASP suite. They were erupted at relatively shallow water depths (950-1350 m). Nonetheless, even at this pressure, the measured water concentrations of <1 wt.% should be water-undersaturated (Fig. 3A). Like the ASP sample suite, only samples with the highest water concentrations could undergo any water loss during degassing of a CO_2 -saturated melt, yet those samples do not have δD values that are lower than other Loihi samples (Figs. 3A, B). Estimates of the water concentrations for a parental magma having Mg# (molecular Mg/ Mg+0.9*Fe) =68 results in a tight cluster of all but two of the Loihi basalts (Fig. 3C). For all but these two samples, there is a narrow range of δD from -70% to -78%, and a small range of H_2O/Ce from 142 to 177 (**Fig. 3D**). These δD values are significantly lower than

322

323

324

325

326

327

328

329

330

331

332

333

334

335

336

337

338

339

340

341

342

343

344

those of the ASP samples having high ${}^{3}\text{He}/{}^{4}\text{He}$ (where δD extends to -50%). The δD

values of -70‰ to -78‰ correspond closely to previous estimates for Hawaii and Loihi (Friedman, 1967; Rison and Craig, 1983; Garcia et al. 1989) and fall in a more restricted range than the δD results from melt inclusions (-79‰ to -118‰ at Loihi, +40‰ to -165‰ at other Hawaiian volcanos, Hauri, 2002). The H₂O/Ce values are also identical to the Loihi value of 167 ± 13 reported by Dixon and Clague (2001).

Two Loihi basalts have lower δD values of -83‰ and -89‰ and significantly lower H_2O/Ce =120. These samples also have the highest vesicularity for the Loihi suite (~40 vol.%; **Table S3**). Their high vesicularity, along with their relatively shallow eruption pressures, suggests that some hydrogen isotope fractionation occurred during the small amount of water loss that would have accompanied their extensive CO_2 degassing (e.g., De Hoog et al., 2009; **Fig. 3B**). This may have occurred under equilibrium degassing conditions, or it may be a disequilibrium phenomenon. Dixon and Clague (2001) noted that disequilibrium between molecular [H_2O] and [OH^-] in Loihi glasses is consistent with small amounts of water diffusion into vesicles. This process might account for the low δD and H_2O/Ce in these two anomalous samples, as well as the greater range of δD in replicate analyses of other Loihi samples

3.3. Global δD variability in submarine basalts

Our new δD values for the SEIR basalts and for Loihi seamount provide two contrasting patterns of water and δD behavior in two different high 3 He/ 4 He sample suites. We consider the implications of these two patterns within a broader global context, using published δD - 3 He/ 4 He that includes the large compilation of δD values from globally

distributed submarine basalts reported in Dixon et al. (2017). Samples from the Azores Platform (North Atlantic), northern East Pacific Rise (EPR) near the Orozco Fracture Zone, and a subset of those from the Easter Microplate and Easter-Salas v Gomez Seamounts were measured by the same TC/EA laboratory and procedure as the ASP and Loihi samples studied here. We also consider *trends* of conventional δD results from the Mid-Atlantic Ridge north and south of Iceland (Poreda et al., 1986), the Easter Microplate and Easter-Salas y Gomez Seamounts (Poreda et al., 1993; Kingsley et al., 2002; revised in Dixon et al., 2017), the Pacific Antarctic Ridge (Clog et al., 2013), and the South Atlantic Discovery and Shona geochemical anomalies (Dixon et al., 2017). As discussed in section 2.2, these conventional δD data may be systematically offset from TC/EA measurements. The overall global compilation of submarine glass δD values measured by TC/EA shows a normal distribution ranging from -98% to -40%, with a mean of -75% ($1\sigma = 12\%$, n =95; **Fig. 5**). Basalts derived from nominally depleted mantle, defined as those having chondrite-normalized (La/Sm)_n <1, have a pattern similar to the overall data set, but their upper limit is -59% (\bar{x} =-81%, n =49). In contrast, enriched mantle basalts with (La/Sm)_n >1 display a pattern resembling a bimodal distribution, with one peak at -70 to -75%, similar to the overall data set, and another peak at -50 to -60% (overall \bar{x} =-68%, n =44). The δD distributions using ³He/⁴He as a discriminant are similar to those based on mantle enrichment. We have chosen 10 R_A as a cutoff value for an approximate upper limit in basalts derived from the depleted mantle (Graham et al., 2014). Basalts having ³He/⁴He

368

369

370

371

372

373

374

375

376

377

378

379

380

381

382

383

384

385

386

387

388

 $<10 \text{ R}_{A}$ are normally distributed with a mean of -73% (n =24), and basalts with ${}^{3}\text{He}/{}^{4}\text{He}$ 390 >10 R_A show two peaks at -70 to -75% and -50 to -55% (overall \bar{x} =-68%, n =24). 391 392 393 Both the SEIR basalt suite and the global submarine data set show that δD is broadly 394 correlated with mantle enrichment factors such as La/Sm, and with long-lived isotopic tracers of enrichment such as ²⁰⁶Pb/²⁰⁴Pb and ⁸⁷Sr/⁸⁶Sr (**Figs. 6, 7, S2**). There is 395 396 considerable scatter as expected when including basalts from many different regions, and 397 some extreme samples lying away from the broad trends are also found (e.g., the highest 398 ⁸⁷Sr/⁸⁶Sr basalts from the South Atlantic and the ASP region of the SEIR; **Fig. 7**). Some 399 individual sample groups show a strong covariation, such as segment H from the SEIR, where δD , La/Sm, and $^{206}Pb/^{204}Pb$ encompass $\sim 75\%$ of the global range along mid-ocean 400 401 ridges (Figs. 2, S1, S2). 402 No global pattern toward higher δD values at high ${}^{3}\text{He}/{}^{4}\text{He}$ ratios is observed (**Fig. 6**). 403 404 Although positive correlations are found within individual sample suites (e.g., ASP, Easter), basalt suites having the highest ³He/⁴He ratios, associated with Iceland and Loihi 405 406 Seamount, have low δD values <-70% (**Fig. 6**). 407 Within individual ocean basins, broad arrays are evident in a diagram of δD vs. ⁸⁷Sr/⁸⁶Sr 408 409 (Fig. 7), as well as for other radiogenic systems (Fig. S2). Within the Easter, North 410 Atlantic, and ASP sample suites, basalts with higher δD values appear to trend toward higher ⁸⁷Sr/⁸⁶Sr. Another noteworthy feature is that MORB compositions having the 411

lowest values of δD (\leq -90‰) appear to converge toward a common value of ${}^{87}Sr/{}^{86}Sr$ near 0.703 (**Fig. 7**).

4. Origins of δD variability in mantle-derived magmas

D/H ratios have greater variability throughout the solar system than any other isotopic ratio (e.g., Marty and Yokochi, 2006). On Earth, δD values appear to be restricted to a normal distribution between -100‰ and -40‰ in mantle-derived basalts (**Fig. 5**; extending to -30‰ if conventional analyses are included). We examine some details of the variations within this range to help better constrain Earth's primordial δD value, and to ascertain the processes that might account for deviations from it.

4.1. δD in high ³He/⁴He basalts

High and low ${}^{3}\text{He}/{}^{4}\text{He}$ basalts span almost the same range of δD (**Fig. 5**). The δD frequency peak around -50‰ observed in high ${}^{3}\text{He}/{}^{4}\text{He}$ basalts is best explained by a surface water component that was recycled by subduction and incorporated into the source of mantle plumes near the core-mantle boundary (**section 4.1.1**). Here the surface water component is assumed to be characterized by $\delta D \sim 0\%$, although values of -7‰ or lower may have been present through much of Earth's history (Lécuyer et al., 1998). This peak is dominated by high ${}^{3}\text{He}/{}^{4}\text{He}$ basalts from the SEIR and from the Easter hotspot region (**Fig. 6**; Kingsley et al., 2002; Dixon et al., 2017). The other δD frequency peak around -75‰ observed in both high and low ${}^{3}\text{He}/{}^{4}\text{He}$ basalts (**Fig. 5**), and similar to the δD peak in depleted basalts distributed globally, may provide the best characterization of

Earth's primordial δD value. It is exemplified by the highest ³He/⁴He submarine glasses from Loihi Seamount (**Fig. 6**, **section 4.1.2**).

Plate tectonic recycling has been recognized for decades as a process of central

4.1.1. Recycled water

importance in the geochemical cycle of water (e.g., Ito et al., 1983; Giggenbach, 1992; Lécuyer et al., 1998; Shaw et al., 2008; Dixon et al., 2017). Basalts from subduction zones and back arc basins include high δD values (up to -20‰), and early models suggested that residual slabs subducted into the mantle should therefore be deuterium-depleted and subduction zone mantle wedge peridotite should be deuterium-enriched (e.g., Poreda et al., 1985; Giggenbach, 1992; Shaw et al., 2008). Dixon et al. (2017), however, proposed that rehydration of a slab by higher pressure mineral dehydration may allow some residual slabs to become deuterium-enriched, as also shown by experimental studies of dehydration in mantle minerals (Roskosz et al, 2018). When subducted into the deep mantle, this D-enriched slab material can be intermixed with other components that comprise the source of mantle plumes. This recycling process can explain high δD values accompanying geochemically-enriched signatures in both mid-ocean ridge and ocean island basalts.

Our δD results for the SEIR basalts, and the enriched ASP sub-group (from segments H, I and J), are consistent with the slab rehydration explanation in the Dixon et al. (2017) model. The ASP lavas have higher water contents, δD values up to -50‰, and elevated $^{206}\text{Pb}/^{204}\text{Pb}$ identical to the C-component of Hanan and Graham (1996). The C-

component (interchangeably referred to by Dixon et al., 2017, as PREMA—for PREvalent MAntle—Zindler and Hart, 1986) was postulated by Hanan and Graham (1996) to originate from recycled oceanic crust of predominantly Proterozoic age (600-2000 Ma). The high ³He/⁴He ratios, up to 14 R_A, of these samples implies that any such recycled material was mixed with a deep mantle component sampled by the ASP plume. This scenario is consistent with evidence from noble gas and radiogenic isotope systematics (White, 2015) and state-of-the-art simulations of mantle convection (Li et al., 2014) that collectively indicate primordial material and subducted lithosphere can mix in or near the plume generation zones associated with the LLSVPs (Large-Low Shear wave Velocity Provinces) at the core-mantle boundary. These recycled materials can subsequently become entrained into a mantle plume. The geochemical arrays for the SEIR basalts are therefore best explained by mixing between ASP plume material (itself a mixture of recycled lithosphere and primordial mantle, see section 4.3), and depleted upper mantle (Fig. 8).

4.1.2. Primordial water

The lower δD mode at Loihi Seamount occurs in high ${}^{3}\text{He}/{}^{4}\text{He}$ basalts that are geochemically less enriched than those from the ASP and Easter hotspots. Comparable δD values also occur in moderately high ${}^{3}\text{He}/{}^{4}\text{He}$ lavas from Iceland (**Fig. 6**). The lower $H_{2}O/Ce$ ratios of Loihi basalts relative to other moderately enriched basalts globally seem to suggest a lower water content in the Loihi mantle source (**Figs. 3 and 7**; Dixon and Clague, 2001), although $H_{2}O/Ce$ may not be as reliable an indicator of water

479 concentration in OIB source mantle compared to MORB source mantle (e.g., Peslier et 480 al., 2017). 481 482 The Dixon et al. (2017) recycling model hypothesizes that the low H_2O and $\delta D = -75\%$ in 483 the Loihi mantle source originates from dehydrated lithosphere of high temperature 484 subducted slabs. This is consistent with the low H₂O/Ce observed in Loihi basalts (Dixon 485 and Clague, 2001). However, such "dry" recycled materials will have a very low 486 proportional contribution of water during mixing with a primordial mantle component 487 (e.g., Marty, 2012). End-member H₂O concentrations are not well known for such mixing 488 scenarios and this makes quantitative modeling of the mixing very uncertain. Although a 489 contribution of some recycled water to the Loihi mantle source is possible, it seems likely 490 that there is a substantial contribution from primordial mantle. The very high ${}^{3}\text{He}/{}^{4}\text{He}$ 491 ratios require the presence of a primordial volatile component, and it must strongly 492 influence, if not dominate, the δD composition of the Loihi source mantle. 493 494 Loihi δD values (-75‰) also resemble those for typical MORB mantle (Fig. 5), an 495 observation noted previously by Kyser and O'Neil (1984) and Garcia et al. (1989). 496 Furthermore, typical partial melting is not expected to lead to large differences in δD 497 between basalts and their source mantle (e.g., Bindeman et al., 2012). Therefore, depleted MORB mantle would have lower concentrations of water and ³He due to their 498 499 incompatible behavior during melting, but its primordial δD composition should be 500 largely unmodified if the mantle region has not been affected by recycled water. 501

A primordial δD value near -75‰ is also similar to δD values of chondritic meteorites (e.g., $-100 \pm 60\%$; Robert, 2003; Alexander, 2017). This supports the common argument that the bulk of Earth's H isotope composition was acquired during the accretion of chondrite-like materials (e.g., Lécuyer et al., 1998; Williams and Hemley, 2001; Marty and Yokochi, 2006; Marty, 2012; Peslier et al., 2017). However, studies of light noble gases (He, Ne) indicate that a solar component may also be present in the deep mantle (Williams and Mukhopadhyay, 2018). A recent planetary modeling study by Wu et al. (2018) considered the effects of hydrogen dissolution into an early magma ocean when solar nebula gas was still present, along with H isotope fractionation during core formation. The study concluded that a small but significant percentage of hydrogen in the deep Earth has a nebular origin, and that the mantle residue of magma ocean crystallization would have had δD values near -110%. Given our limited number of δD analyses in Loihi basalts, all of which were collected near the summit, further study of deeper, less degassed submarine basalts from Loihi seamount will likely prove to be important for precisely establishing the primordial value of δD . The Loihi submarine glass results appear to provide evidence counter to the proposed primordial δD of <-200% based on δD of melt inclusions from high ${}^{3}\text{He}/{}^{4}\text{He}$ basalts at Baffin Island (Hallis et al., 2015). Melt inclusions may be modified from primary mantle values by diffusive hydrogen exchange through host olivine crystals with water enriched melts (Portnyagin et al., 2008; Gaetani et al., 2012). This process may result in anomalously low δD values (Hauri, 2002; Michael, 2017; Gatti et al., 2018). The Loihi

502

503

504

505

506

507

508

509

510

511

512

513

514

515

516

517

518

519

520

521

522

basalt data provide evidence that primordial He isotope signatures in deep mantle plume source regions may be accompanied by δD values near -75%.

526

527

528

529

530

531

532

533

534

535

536

537

538

539

540

541

542

543

524

525

4.2. Depleted δD endmember

The δD values that extend to -100% cannot be explained by mixing between primordial water having $\delta D = -75\%$ and surface water having $\delta D \sim 0\%$. The low δD limit is similar in all ocean basins (Mid-Atlantic Ridge Azores Plateau, Northern East Pacific Rise, and Southeast Indian Ridge) and it also converges at a common value of ⁸⁷Sr/⁸⁶Sr near 0.703 (Figs. 3 and 7). One possible explanation is that extreme refinement of the mantle source of the ultra-depleted ridge basalts due to multiple episodes of melt extraction has led to the observed low water concentrations and a lower (fractionated) δD value. Hydrogen isotope fractionation is usually assumed to be insignificant during the partial melting process (e.g., Kyser and O'Neil, 1984). However, Bindeman et al. (2012) calculated that when melt fractions are low (<1-2%) the melt could have a higher δD value than the source peridotite. This occurs because molecular water that preferentially partitions into the melt is relatively higher in its D/H ratio, while hydrogen that remains in residual anhydrous minerals is relatively lower in D/H. After several percent melting, nearly all the hydrogen will have been incorporated into the melt fraction, leaving little leverage for any D/H fractionation during further melting. Residual mantle porosity during melting is <1% based on U-series disequilibria (e.g.,

544

545

546

Beattie, 1993) and so the partial melting process is a near fractional one and water will be

effectively scavenged from the mantle source. Small amounts of hydrogen might be retained in the mantle, however, either as (1) H_2O and OH^- in any residual melt that is not squeezed out during an extraction event, or as (2) minor amounts of hydrogen in nominally anhydrous phases in the mantle (e.g., Bell and Ihinger, 2000). Any residual melts would have the same δD as extracted melts, but H^+ in residual solids can have significantly lower δD (Bell and Ihinger, 2000). Therefore, melts derived from a separate, later melting event involving previously melted mantle, such as the source of ultradepleted MORB (e.g., Michael and Graham, 2015; Graham et al., 2016), may have the potential to be shifted to lower δD values. More experimental and modeling work is needed to test this idea.

4.3. Mixing of δD between endmembers

Three terrestrial endmember δD compositions are identified here: $\sim 0\%$ (surface water), -75% (primordial water), and -100% (low D/H water, potentially produced by isotopic fractionation during small extents of melting). Mixing proportions in different mantle sources can be estimated from these values.

The highest δD values in the ASP basalt suite suggest that recycled water dominates the signal over primordial water in that region. For example, if the recycled end-member δD is -20% (the mantle wedge from beneath arc lavas, e.g., Shaw et al., 2008), then the measured values of -50% in ASP basalts imply that roughly 40% of the H₂O has a recycled origin (assuming a primordial end-member δD of -75%). This argument can extend to He isotopes: the highest ${}^{3}\text{He}/{}^{4}\text{He}$ ratios in the ASP sample suite are 14 R_A,

intermediate between recycled slab compositions ($<6~R_A$) and higher values characteristic of mantle plume sources beneath Hawaii and Iceland ($>30~R_A$). Modestly high $^3He/^4He$ of 15-20 R_A may result from entrainment and mixing together of primitive and recycled materials (Gonnermann and Mukhopadhyay, 2009).

The depleted end-member δD values that approach -100% might be caused by >30% contribution of D/H-depleted nominally anhydrous minerals to residual melt from a MORB source. Mid-ocean ridge basalts that have $(La/Sm)_n < 1$ are offset in δD toward this depleted end-member from primordial values (-75%), suggesting some influence of nominally anhydrous minerals. Many parts of the MORB mantle, however, have δD values that are remarkably similar to -75% and identical to the δD value of high 3 He/ 4 He Loihi samples. This similarity suggests that much of the Earth's mantle still contains a significant component of juvenile water.

5. Conclusions

The lowest δD values in submarine basalts (-90 to -100‰) are found in trace element depleted MORB glasses having $(La/Sm)_n < 1$ and roughly similar $^{87}Sr/^{86}Sr = 0.703$. This depleted end-member composition potentially results from a multi-stage history of melt extraction (e.g., Michael and Graham, 2015; Graham et al., 2016), during which a small amount of D/H-depleted hydrogen may have been retained within nominally anhydrous minerals in the (residual) mantle that was ultimately melted at a later time.

Submarine basalts with higher δD values are associated with enriched geochemical signatures, such as elevated La/Sm. All submarine basalt glasses with $\delta D >-55\%$ have $(\text{La/Sm})_n >1$. These enriched, high δD basalts originate from a mantle source that contains a subduction component of water. The correlation of high $^3\text{He/}^4\text{He}$ with δD enrichment in the ASP hotspot-influenced basalts is evidence that the subducted hydrous material was transported into the lower mantle, where it was subsequently entrained into a mantle plume that also tapped a primordial reservoir (**Fig. 8**).

Most δD values for submarine basalt glasses distributed globally lie in a narrow range of -75 ±12‰ (1 σ , n=95). Submarine basalt glasses having high 3 He/ 4 He ratios from Loihi Seamount also have δD =-73 ±12‰ and are indistinguishable from the global average. In contrast to the dominantly recycled δD signature that trends to -50‰ in ASP hotspot basalts having high 3 He/ 4 He ratios, the δD values from Loihi Seamount arguably provide a current best estimate for Earth's primordial δD . Some high 3 He/ 4 He mantle source regions appear to still contain a significant component of their primordial water.

Acknowledgments

We appreciate thoughtful and constructive reviews by Cyril Aubaud, Anne Peslier, and Mark Stelten, as well as editorial handling by Frederic Moynier. We thank Jim Palandri for assistance with hydrogen isotope analyses and Jackie Dixon for graciously sharing compilation data tables from her work. Initial funding for MWL and for δD analyses were provided by NSF EAR 1447337. Additional analytical work was supported by NSF

614 support of DWG by OCE 1357061 and OCE 1558798. INB acknowledges support by 615 EAR 1822977. 616 617 **References Cited** 618 Alexander, C.M.O., 2017. The origin of inner Solar System water. Phil. Trans. R. Soc. A 619 375, 20150384–20. doi:10.1098/rsta.2015.0384 620 Allègre, C.J., Staudacher, T., Sarda, P., Kurz, M., 1983. Constraints on evolution of 621 Earth's mantle from rare gas systematics. Nature 303, 762–766. 622 doi:10.1038/303762a0 623 Aubaud, C., Hauri, E.H., Hirschmann, M.M., 2004. Hydrogen partition coefficients 624 between nominally anhydrous minerals and basaltic melts. Geophysical Research 625 Letters 31, L20611. doi:10.1029/2004GL021341 626 Beattie, P., 1993. Uranium–thorium disequilibria and partitioning on melting of garnet 627 peridotite. Nature 363, 63–65. doi:10.1038/363063a0 628 Bell, D.R., Ihinger, P.D., 2000. The isotopic composition of hydrogen in nominally 629 anhydrous mantle minerals. Geochimica et Cosmochimica Acta 64, 2109-2118. 630 Bindeman, I.N., Kamenetsky, V.S., Palandri, J., Vennemann, T., 2012. Hydrogen and 631 oxygen isotope behaviors during variable degrees of upper mantle melting: Example 632 from the basaltic glasses from Macquarie Island. Chemical Geology 310-311, 126-633 136. doi:10.1016/j.chemgeo.2012.03.031 634 Clog, M., Aubaud, C., Cartigny, P., Dosso, L., 2013. The hydrogen isotopic composition 635 and water content of southern Pacific MORB: A reassessment of the D/H ratio of the

- depleted mantle reservoir. Earth and Planetary Science Letters 381, 156–165.
- 637 doi:10.1016/j.epsl.2013.08.043
- 638 Clog, M., Cartigny, P., Aubaud, C., 2012. Experimental evidence for interaction of water
- vapor and platinum crucibles at high temperatures: Implications for volatiles from
- igneous rocks and minerals. Geochimica et Cosmochimica Acta 83, 125–137.
- 641 Craig, H., Lupton, J.E., 1976. Primordial neon, helium, and hydrogen in oceanic basalts.
- Earth and Planetary Science Letters 31, 369–385.
- De Hoog, J.C.M., Taylor, B.E., Van Bergen, M.J., 2009. Hydrogen-isotope systematics in
- degassing basaltic magma and application to Indonesian arc basalts. Chemical
- Geology 266, 256–266. doi:10.1016/j.chemgeo.2009.06.010
- Dixon, J.E., Bindeman, I.N., Kingsley, R.H., Simons, K.K., Le Roux, P.J., Hajewski,
- T.R., Swart, P., Langmuir, C.H., Ryan, J.G., Walowski, K.J., Wada, I., Wallace, P.J.,
- 2017. Light Stable Isotopic Compositions of Enriched Mantle Sources: Resolving the
- Dehydration Paradox. Geochemistry, Geophysics, Geosystems 18, 1–39.
- doi:10.1002/2016GC006743
- Dixon, J.E., Clague, D.A., 2001. Volatiles in Basaltic Glasses from Loihi Seamount,
- Hawaii: Evidence for a Relatively Dry Plume Component. Journal of Petrology 42,
- 653 627–654.
- Douglas-Priebe, L.M., 1998, Geochemical and petrogenetic effects of the interaction of
- 655 the Southeast Indian Ridge and the Amsterdam-Saint Paul hotspot, M.S. thesis,
- Oregon State University, Corvallis. 132 p.
- Friedman, I., 1967. Water and deuterium in pumice from the 1959-60 eruption of Kilauea
- Volcano, Hawaii. U.S. Geological Survey Professional Paper 575-B, 120–127.

- 659 Gaetani, G.A., O'Leary, J.A., Shimizu, N., Bucholz, C.E., Newville, M., 2012. Rapid
- reequilibration of H₂O and oxygen fugacity in olivine-hosted melt inclusions.
- Geology 40, 915-918. doi:10.1130/G32992.1
- Garcia, M.O., Jorgenson, B.A., Mahoney, J.J., 1993. An evaluation of temporal
- geochemical evolution of Loihi summit lavas: Results from *Alvin* Submersible Dives.
- Journal of Geophysical Research 98, 537–550.
- Garcia, M.O., Muenow, D.W., Aggrey, K.E., O'Neil, J.R., 1989. Major element, volatile,
- and stable isotope geochemistry of Hawaiian submarine tholeitic glasses. Journal of
- 667 Geophysical Research 94, 10525–10538.
- Garcia, M.O., Rubin, K.H., Norman, M.D., Rhodes, J.M., Graham, D.W., Muenow, D.,
- Spencer, K., 1998. Petrology and geochronology of basalt breccia from the 1996
- earthquake swarm of Loihi seamount, Hawaii: magmatic history of its 1996 eruption.
- Bulletin of Volcanology 59, 577–592.
- 672 Gatti, E., Bucholz, C., Guan, Y., Zhang, Y., Gaetani, G., Eiler, J., 2018. δD variations in
- olivine-hosted melt inclusions due to post-entrapment processes: A case study from
- Baffin Island picrites. Goldschmidt Abstracts, p. 798.
- 675 Giggenbach, W.F., 1992. Isotopic shifts in waters from geothermal and volcanic systems
- along convergent plate boundaries and their origin. Earth and Planetary Science
- 677 Letters 113, 495–510.
- 678 Gonnermann, H.M., Mukhopadhyay, S., 2009. Preserving noble gases in a convecting
- 679 mantle. Nature 459, 560–563. doi:10.1038/nature08018

- 680 Graham, D.W., Hanan, B.B., Hémond, C., Blichert-Toft, J., Albarède, F., 2014. Helium
- isotopic textures in Earth's upper mantle. Geochemistry, Geophysics, Geosystems 15,
- 682 2048–2074. doi:10.1002/2014GC005264
- 683 Graham, D.W., Jenkins, W.J., Kurz, M.D., Batiza, R., 1987. Helium isotope
- disequilibrium and geochronology of glassy submarine basalts. Nature 326, 384–386.
- 685 doi:10.1038/326384a0
- 686 Graham, D.W., Johnson, K., Douglas Priebe, L., Lupton, J.E., 1999. Hotspot-ridge
- interaction along the Southeast Indian Ridge near Amsterdam and St. Paul islands:
- helium isotope evidence. Earth and Planetary Science Letters 167, 297–310.
- 689 Graham, D.W., Michael, P.J., Shea, T., 2016. Extreme incompatibility of helium during
- mantle melting: Evidence from undegassed mid-ocean ridge basalts. Earth and
- 691 Planetary Science Letters 454, 192-202. doi:10.1016/j.epsl.2016.09.016
- Hallis, L.J., Huss, G.R., Nagashima, K., Taylor, G.J., Halldórsson, S.A., Hilton, D.R.,
- Mottl, M.J., Meech, K.J., 2015. Evidence for primordial water in Earth's deep mantle.
- 694 Science 350, 795–797. doi:10.1126/science.aac4834
- Hanan, B.B., Graham, D.W., 1996. Lead and Helium Isotope Evidence from Oceanic
- Basalts for a Common Deep Source of Mantle Plumes. Science 272, 991–995.
- 697 doi:10.1126/science.272.5264.991
- Hart, S.R., 1984. A large-scale isotope anomaly in the Southern Hemisphere mantle.
- 699 Nature 309, 753–757. doi:10.1038/309753a0
- Hauri, E.H., 2002. SIMS analysis of volatiles in silicate glasses, 2: isotopes and
- abundances in Hawaiian melt inclusions. Chemical Geology 183, 115–141.
- Hirschmann, M.M., 2006, Water, melting, and the deep Earth H₂O cycle. Annual

- Reviews in Earth and Planetary Science 34, 629-653.
- Honda, M., McDougall, I., Patterson, D., Doulgeris, A., Clague, D.A., 1993. Noble gases
- in submarine pillow basalt glasses from Loihi and Kilauea, Hawaii: a solar
- component in the Earth. Geochimica et Cosmochimica Acta 57, 859–874.
- 707 Ito, E., Harris, D.M., Anderson, A.T., Jr., 1983. Alteration of oceanic crust and geologic
- 708 cycling of chlorine and water. Geochimica et Cosmochimica Acta 47, 1613–1624.
- 709 doi:10.1016/0016-7037(83)90188-6
- Johnson, K.T.M., Graham, D.W., Rubin, K.H., Nicolaysen, K., Scheirer, D.S., Forsyth,
- D.W., Baker, E.T., Douglas-Priebe, L.M., 2000. Boomerang Seamount: the active
- expression of the Amsterdam–St. Paul hotspot, Southeast Indian Ridge. Earth and
- 713 Planetary Science Letters 183, 245–259. doi:10.1016/S0012-821X(00)00279-X
- Kent, A.J., Clague, D.A., Honda, M., Stolper, E.M., Hutcheon, I., Norman, M.D., 1999.
- 715 Widespread assimilation of a seawater-derived component at Loihi Seamount,
- Hawaii. Geochimica et Cosmochimica Acta 63, 2749–2761.
- Kingsley, R.H., Schilling, J.-G., Dixon, J.E., Swart, P., Poreda, R., Simons, K., 2002.
- D/H ratios in basalt glasses from the Salas y Gomez mantle plume interacting with
- the East Pacific Rise: Water from old D-rich recycled crust or primordial water from
- the lower mantle? Geochemistry, Geophysics, Geosystems 3, 1–26.
- 721 doi:10.1029/2001GC000199
- Kurz, M.D., Jenkins, W.J., Hart, S.R., 1982. Helium isotopic systematics of oceanic
- islands and mantle heterogeneity. Nature 297, 43–46.

- Kurz, M.D., Jenkins, W.J., Hart, S.R., Clague, D., 1983. Helium isotopic variations in
- volcanic rocks from Loihi Seamount and the Island of Hawaii. Earth and Planetary
- 726 Science Letters 66, 388–406. doi:10.1016/0012-821X(83)90154-1
- 727 Kyser, T.K., O'Neil, J.R., 1984. Hydrogen isotope systematics of submarine basalts.
- Geochimica et Cosmochimica Acta 48, 2123-2133.
- Lécuyer, C., Gillet, P., Robert, F., 1998. The hydrogen isotope composition of seawater
- and the global water cycle. Chemical Geology 145, 249–261.
- Li, M., McNamara, A.K., Garnero, E.J., 2014. Chemical complexity of hotspots caused
- by cycling oceanic crust through mantle reservoirs. Nature Geoscience 7, 366–370.
- 733 doi:10.1038/ngeo2120
- Loewen, M.W., Kent, A.J., 2012. Sources of elemental fractionation and uncertainty
- during the analysis of semi-volatile metals in silicate glasses using LA-ICP-MS.
- Journal of Analytical Atomic Spectrometry 27, 1502–1508. doi:10.1039/c2ja30075c
- Martin E, Bindeman I.N., Balan E., Palandri J., Seligman A., Villemant B.,
- 738 2017. Hydrogen isotope determination by TC/EA technique in application to
- volcanic glass as a window into secondary hydration. Journal of Volcanology and
- 740 Geothermal Research 348, 49-61. doi:10.1016/j.jvolgeores.2017.10.013
- Marty, B., 2012. The origins and concentrations of water, carbon, nitrogen and noble
- gases on Earth. Earth and Planetary Science Letters 313-314, 56–66.
- 743 doi:10.1016/j.epsl.2011.10.040
- Marty, B., Yokochi, R., 2006. Water in the early Earth. Reviews in Mineralogy and
- 745 Geochemistry 62, 421-450.
- 746 McGovern, J., Schubert, G., 1989. Thermal evolution of the Earth: effects of volatile

747 exchange between atmosphere and interior. Earth and Planetary Science Letters 96, 748 27-37. 749 Michael, P.J., 2017. Low D/H in Baffin Island Melt Inclusions: Primordial Water or 750 Diffusive Hydration of Inclusions? Goldschmidt Abstracts, p. 2712. 751 Michael, P.J., Cornell, W.C., 1998. Influence of spreading rate and magma supply on 752 crystallization and assimilation beneath mid-ocean ridges: Evidence from chlorine 753 and major element chemistry of mid-ocean ridge basalts. Journal of Geophysical 754 Research 103, 18325–18356. doi:10.1029/98JB00791 755 Michael, P.J., Graham, D.W., 2015. The behavior and concentration of CO₂ in the 756 suboceanic mantle: Inferences from undegassed ocean ridge and ocean island basalts. 757 Lithos 236-237, 338-351. doi:10.1016/j.lithos.2015.08.020 Moore, J.G, Clague, D.A., Normark, W.R., 1982. Diverse basalt types from Loihi 758 759 seamount, Hawaii. Geology 10, 88-92. 760 Mukhopadhyay, S., 2012. Early differentiation and volatile accretion recorded in deep-761 mantle neon and xenon. Nature 486, 101-104. doi:10.1038/nature11141 762 Newman, S., Lowenstern, J.B., 2002. VolatileCalc: a silicate melt–H₂O–CO₂ solution model written in Visual Basic for excel. Computers & Geosciences 28, 597–604. 763 764 Nicolaysen, K.P., Frey, F.A., Mahoney, J.J., Johnson, K.T.M., Graham, D.W., 2007. 765 Influence of the Amsterdam/St. Paul hot spot along the Southeast Indian Ridge 766 between 77° and 88°E: Correlations of Sr, Nd, Pb, and He isotopic variations with 767 ridge segmentation. Geochemistry, Geophysics, Geosystems 8, 1–24.

768

doi:10.1029/2006GC001540

- Parai, R., Mukhopadhyay, S., 2012. How large is the subducted water flux? New
- constraints on mantle regassing rates. Earth and Planetary Science Letters 317-318,
- 771 396-406.
- Peslier, A.H., Schönbächler, M., Busemann, H., Karato, S.I., 2017. Water in the Earth's
- 773 Interior: Distribution and Origin. Space Science Reviews 212, 743-810.
- 774 doi:10.1007/s11214-017-0387-z.
- Pietruszka, A.J., Keyes, M.J., Duncan, J.A., Hauri, E.H., Carlson, R.W., Garcia, M.O.,
- 2011. Excesses of seawater-derived 234U in volcanic glasses from Loihi Seamount
- due to crustal contamination. Earth and Planetary Science Letters 304, 280-289.
- 778 doi:10.1016/j.epsl.2011.02.018
- Poreda, R., 1985. Helium-3 and deuterium in back-arc basalts: Lau Basin and the
- 780 Mariana Trough. Earth and Planetary Science Letters 73, 244–254.
- 781 doi:10.1016/0012-821X(85)90073-1
- Poreda, R., Schilling, J.G., Craig, H., 1986. Helium and hydrogen isotopes in ocean-ridge
- basalts north and south of Iceland. Earth and Planetary Science Letters 78, 1–17.
- Poreda, R.J., Schilling, J.G., Craig, H., 1993. Helium isotope ratios in Easter microplate
- basalts. Earth and Planetary Science Letters 119, 319–329.
- Portnyagin, M., Almeev, R., Matveev, S., Holtz, F., 2008. Experimental evidence for
- rapid water exchange between melt inclusions in olivine and host magma. Earth and
- 788 Planetary Science Letters 272, 541-552. doi:10.1016/j.epsl.2008.05.020
- Qi, H., Colen, T.B., Gehre, M., Vennermann, T.W., Brand, W.A., Geilmann, H., Olack,
- G., Bindeman, I.N., Palandri, J., Huang, L., Longstraffe, F.J., 2017. New biotite and

- muscovite isotopic reference materials, USGS57 and USGS58, for δ^2 H
- measurements- A replacement for NBS 30. Chemical Geology 467, 89-99.
- 793 Qi, H., Coplen, T.B., Olack, G.A., Vennemann, T.W., 2014. Caution on the use of NBS
- 30 biotite for hydrogen-isotope measurements with on-line high-temperature
- conversion systems. Rapid Communication in Mass Spectrometry 28, 1987–1994.
- 796 doi:10.1002/rcm.6983
- 797 Qi, H., Gröning, M., Coplen, T.B., Buck, B., Mroczkowski, S.J., Brand, W.A., Geilmann,
- H., Gehre, M., 2010. Novel silver-tubing method for quantitative introduction of
- water into high-temperature conversion systems for stable hydrogen and oxygen
- isotopic measurements. Rapid Communication in Mass Spectrometry 24, 1821–1827.
- 801 doi:10.1002/rcm.4559
- Roskosz, M., Deloule, E., Ingrin, J., Depecker, C., Laporte, D., Merkel, S., Remusat, L.,
- Leroux, H., 2018. Kinetic D/H fractionation during hydration and dehydration of
- silicate glasses, melts and nominally anhydrous minerals. Geochimica
- 805 Cosmochemica *Acta 233*, 14-32. doi:10.1016/j.gca.2018.04.027.
- Rison, W., Craig, H., 1983. Helium isotopes and mantle volatiles in Loihi Seamount and
- Hawaiian Island basalts and xenoliths. Earth and Planetary Science Letters 66, 407–
- 808 426.
- Robert, F., 2003. The D/H ratio in chondrites. Space Science Reviews 106, 87-101.
- 810 Sharp., Z.D., Atudorei, V., Durakiewicz, T., 2001. A rapid method for determination of
- hydrogen and oxygen isotope ratios from water and hydrous minerals. Chemical
- 812 Geology 178, 197-210.

813 Shaw, A.M., Hauri, E.H., Fischer, T.P., Hilton, D.R., Kelley, K.A., 2008. Hydrogen 814 isotopes in Mariana arc melt inclusions: Implications for subduction dehydration and 815 the deep-Earth water cycle. Earth and Planetary Science Letters 275, 138–145. 816 doi:10.1016/j.epsl.2008.08.015 817 White, W.M., 2015. Isotopes, DUPAL, LLSVPs, and Anekantavada. Chemical Geology 818 419, 10–28. doi:10.1016/j.chemgeo.2015.09.026 819 Williams, Q., Hemley, R.J., 2001. Hydrogen in the deep Earth. Annual Review of Earth 820 and Planetary Sciences 29, 365-418. 821 Williams, Q., Mukhopadhyay, S., 2018. Capture of nebular gasses during Earth's 822 accretion is preserved in deep-mantle neon. Nature, in press. Doi:10.1038/s41586-823 018-0771-1 824 Zindler, A., Hart, S., 1986. Chemical Geodynamics. Annual Review of Earth and 825 Planetary Sciences 14, 493-571.

Figures

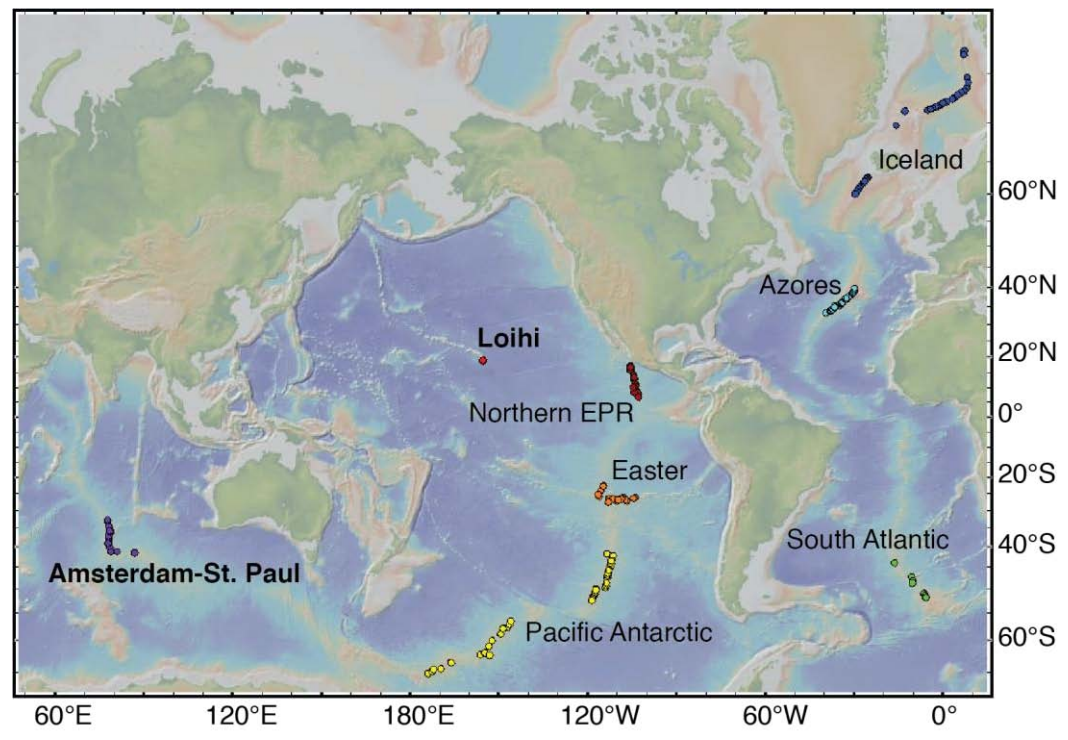


Figure 1. Map showing the distribution of submarine basalt glasses from mid-ocean ridges and ocean islands analyzed for δD . New analyses are from the Amsterdam-St. Paul Plateau and Southeast Indian Ridge, and from Loihi seamount on the flank of Hawaii. Previous δD analyses by identical methods to this study (TC/EA, University of Oregon)—from the Northern EPR, Azores, and Easter—are reported in Dixon et al. (2017). Other δD analyses measured with conventional manometry are included for Easter, Iceland, and the South Atlantic by Dixon et al. (2017), and for the Pacific-Antarctic Ridge by Clog et al. (2013). [1.5 column width.]

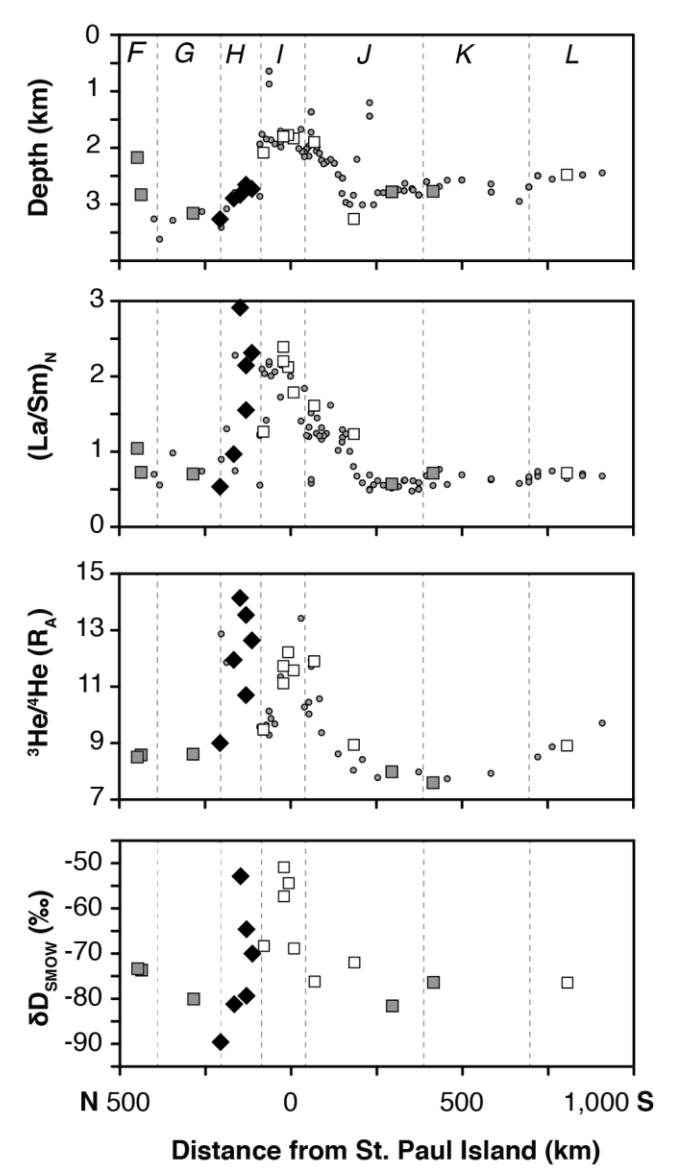


Figure 2. Variations in axial depth (km), chondrite-normalized La/Sm, 3 He/ 4 He (R_A) and δD_{SMOW} (‰) vs. along-axis distance (km) for submarine basalts from the Southeast Indian Ridge in the vicinity of the Amsterdam-St. Paul Plateau (ASP). Divisions between the different ridge segments F through L are shown by vertical dashed lines. Filled gray squares and all segment H diamonds designate samples with MgO >7.5 wt.%, outlined squares have MgO <7.5 wt.%. Small circles designate other samples that were not analyzed for δD. The geochemical anomaly associated with the shallower ridge axis atop the plateau (segments I, J) are also found in segment H (diamonds) ~100 km to the northeast in an area with no depth anomaly. Helium isotope data are from Nicolaysen et al. (2007) and Graham et al. (1999). [1 column width.]

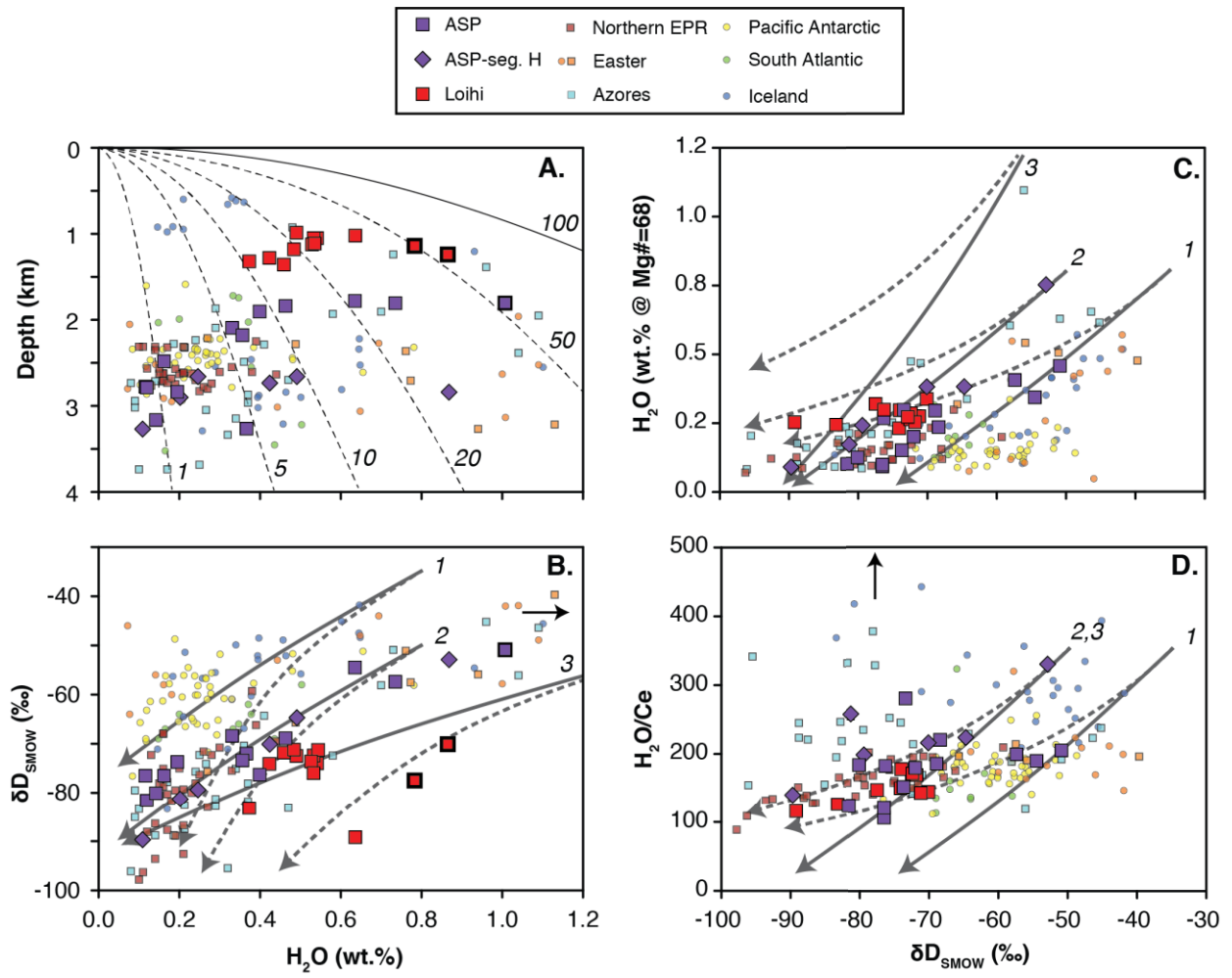


Figure 3. Sample water concentrations compared to (A) depth of sample recovery at the seafloor, and (B) δD . Sample δD compared to (C) water concentrations corrected for crystal fractionation, and (D) H₂O/Ce. Solid line in (A) corresponds to vapor saturation of H₂O in a basaltic melt at 1200°C, while dashed lines show variations in the molar % H₂O with depth for a H₂O-CO₂ equilibrium saturated fluid (calculated in VolatileCalc, Newman and Lowenstern, 2002). In (B), lines correspond to the hydrogen isotope shift during closed-system (solid) vs. open-system (dashed) degassing for three different initial conditions: 0.8 wt.% H₂O and -35‰ (1) or -50% (2), and 1.5 wt.% H₂O and -50% (3). The calculated vapor-melt fractionation follows the model of De Hoog et al. (2009) for a basaltic magma. The three samples from this study that lie closest to saturation are highlighted in a thicker black outline. Each of these samples lie near the highest H₂O and δD for their respective sample suites, so degassing cannot explain their relative positions. The same degassing curves are shown in (C) for the water concentrations corrected for crystal fractionation to primary melt values of Mg# =68, following Michael and Graham (2015), and in (**D**) against H₂O/Ce, which is expected to be constant with different degrees of crystal fractionation and partial melting. Arrows in (B) and (D) denote some samples from Iceland and Easter datasets excluded due to unusually high water and/or H₂O/Ce. Note that for previously published δD data (in Clog et al., 2013; Dixon et al., 2018), samples shown as squares were measured by TC/EA, directly comparable to this work, and samples shown as circles were measured by conventional methods. [2 column width]

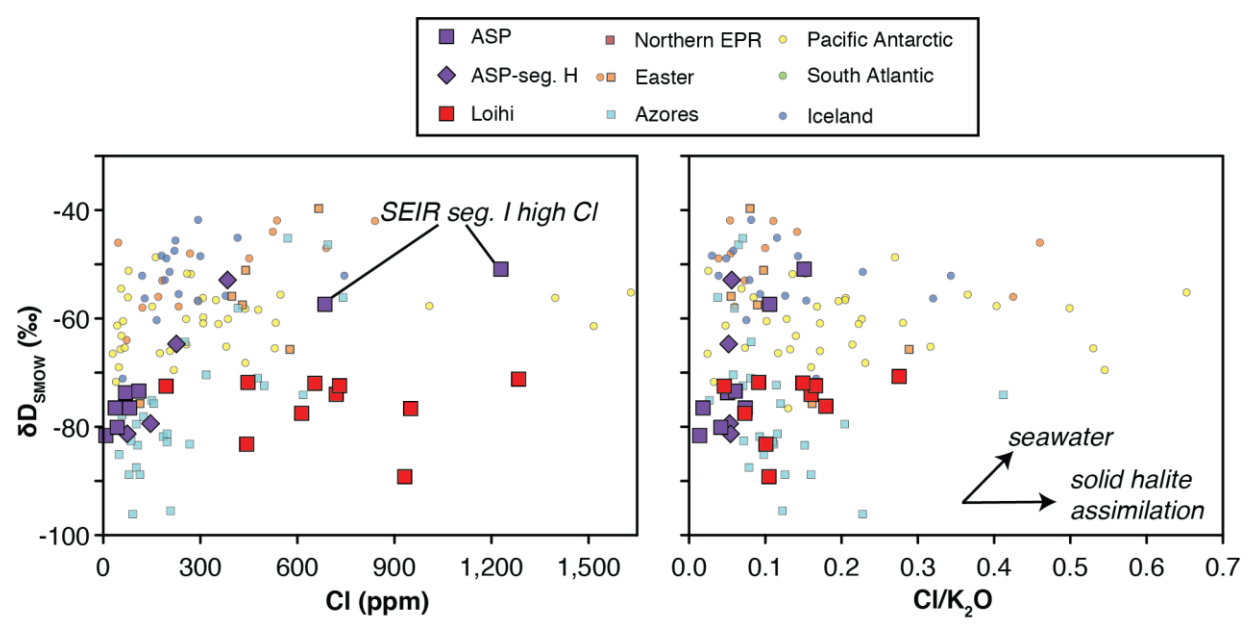


Figure 4. δD vs.[Cl] and Cl/K₂O in suites of submarine basalts distributed globally. [Cl] broadly covaries with δD in the ASP sample suite; however, globally there is no clear trend. Cl/K₂O shows no clear trends. Assimilation or contamination by seawater would result a trend toward δD =0%. The relatively flat trend to high Cl/K₂O instead suggests possible interaction with a highly saline brine or solid halite for the most Cl-enriched basalts. Symbols are the same as **Fig. 3**. [2 column width]

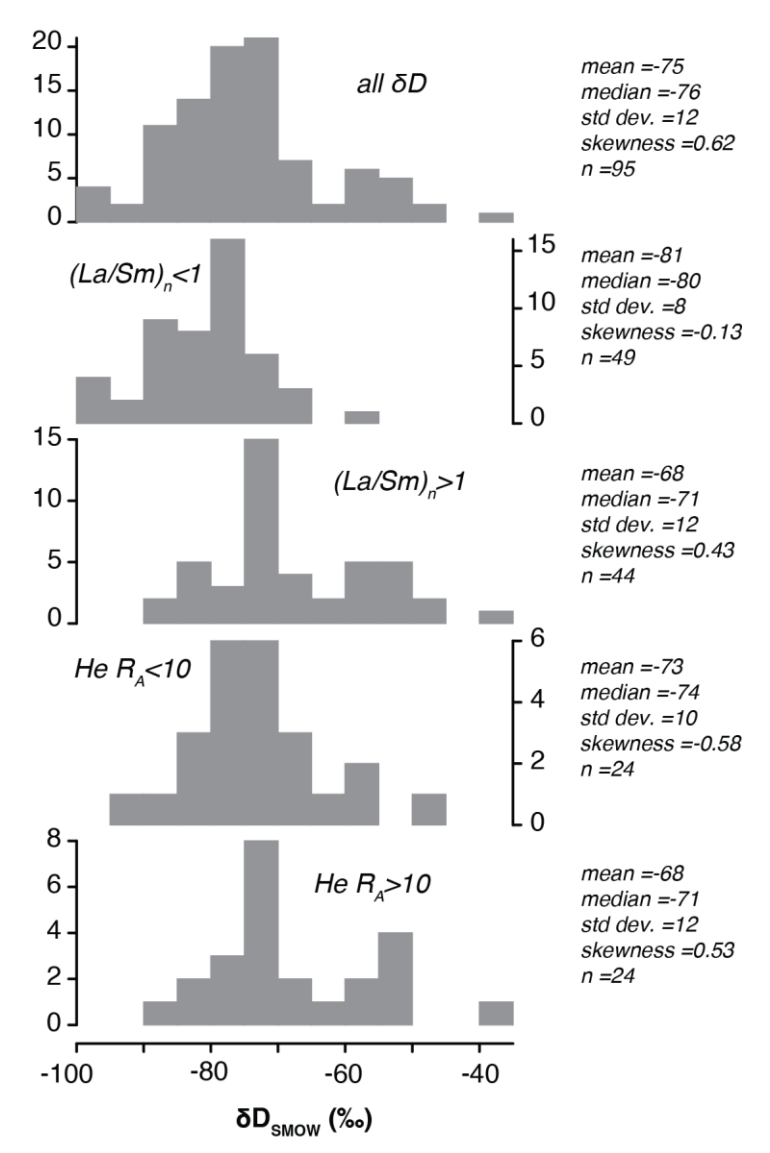


Figure 5. Frequency distribution of δD values measured in submarine glasses by TC/EA. Data are from this study and Dixon et al. (2017). The δD results are normally distributed, with 50% of the samples lying between -65 and -80‰. Depleted mantle samples with $(La/Sm)_n < 1$, have a similar normal distribution but are offset to lower δD with no values greater than -55‰. Samples with enriched mantle signatures, $(La/Sm)_n > 1$, resemble a bimodal distribution having one proportion of the population offset to δD near -50 to -60, and some values as high as <-40‰. Similar distributions are observed for the more limited subset of samples with measured 3 He/ 4 He ratios. Typical MORB mantle samples having 3 He/ 4 He <10 R_A show a normal distribution with a peak around -70%, while samples having elevated 3 He/ 4 He >10 R_A show a bimodal pattern. [1.5 column width]

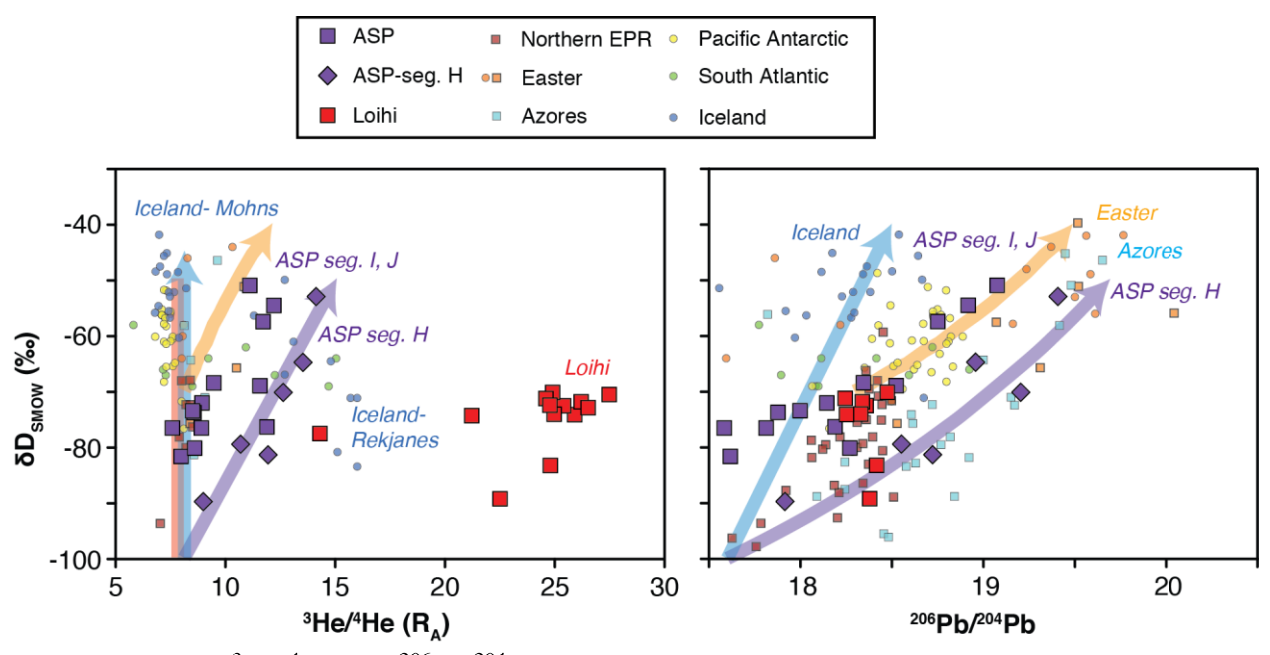


Figure 6. δD vs. 3 He/ 4 He and 206 Pb/ 204 Pb in suites of submarine basalts distributed globally. There is a generally positive covariation between δD and 3 He/ 4 He at the ridge segment scale along the Southeast Indian Ridge (ASP) (segment H, I and J; see also **Fig. 2**). Globally, however, there is no simple trend of δD with helium isotope compositions. Basalts having 3 He/ 4 He <10 R_A extend to the highest δD values, while basalts having the highest 3 He/ 4 He values (from Loihi seamount and also the Reykjanes Ridge) have lower δD of -70 to -90‰. Pb isotopes, as well as other mantle enrichment factors (e.g., La/Sm, K/Ti), show a general positive trend with δD that is best observed within individual sample suites (e.g., ASP segment H). Symbols are the same as **Figs. 3** and **4**. Colored lines represent model mixing curves chosen to highlight trends in the regional data sets. Details of the mixing calculations are provided in the **supplemental material**. [2 column width]

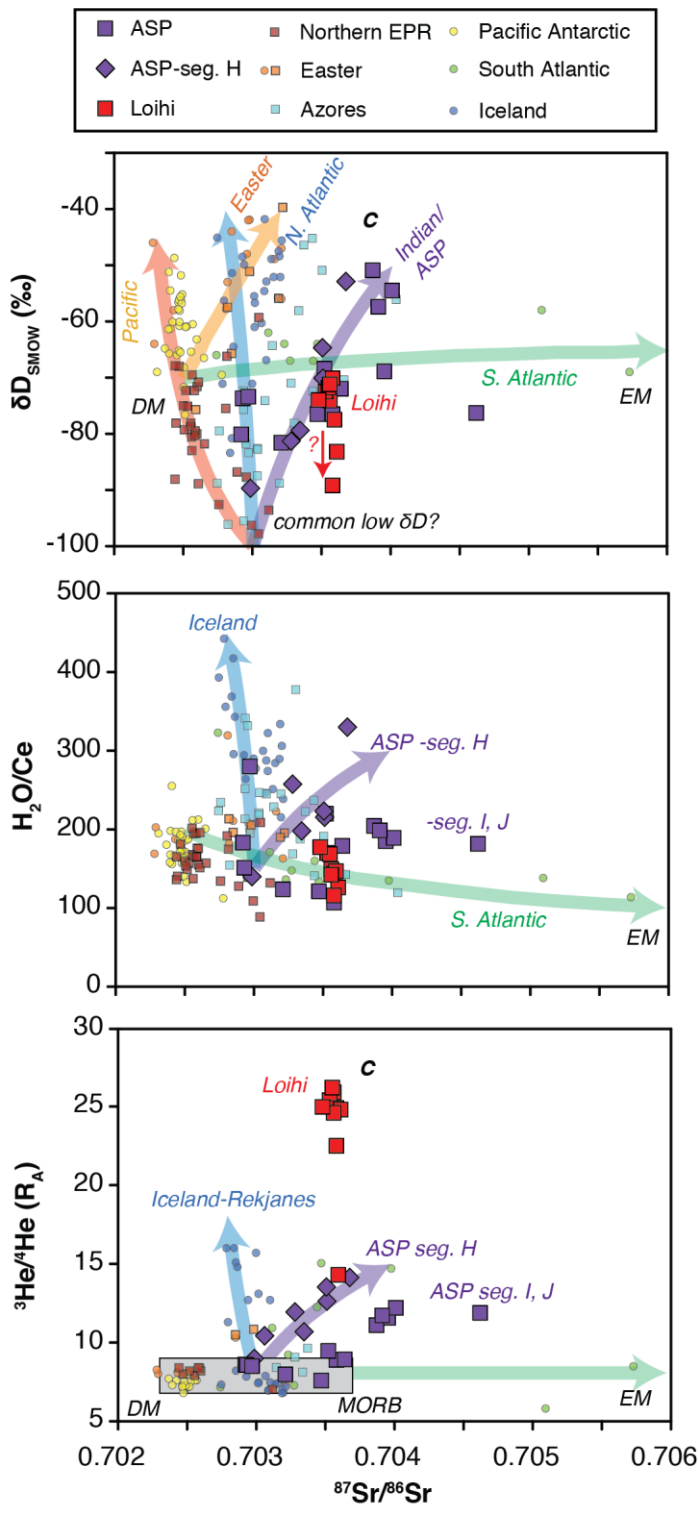


Figure 7. δD, H₂O/Ce, and ³He/⁴He vs. ⁸⁷Sr/⁸⁶Sr in suites of submarine basalts distributed globally. There are major differences in regional trends in these geochemical tracers with respect to Sr isotopes. Broad differences between major ocean basins, previously described by Dixon et al. (2017), can also be matched to mantle chemical domains: depleted mantle (DM), enriched mantle (EM), and common mantle (C, also referred to as PREMA). Gray box shows the typical MORB range, other symbols are the same as **Fig. 3, 4, 6,** and **7**. [1 column width]

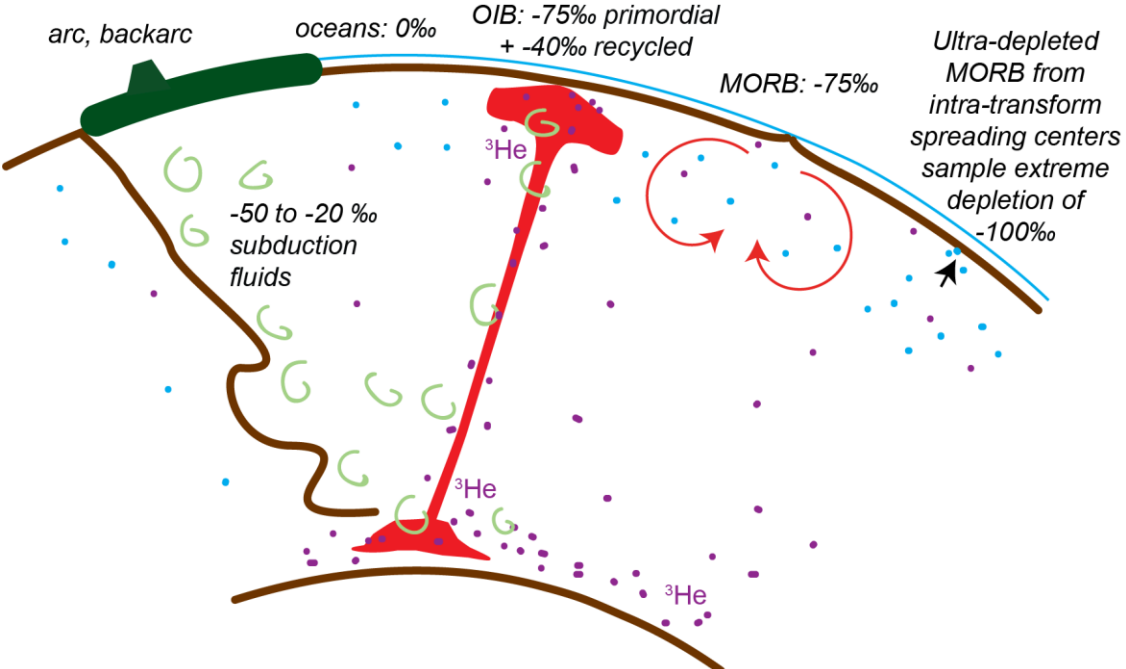


Figure 8. Schematic diagram of possible mantle sources/processes accounting for the range of δD values in submarine basalt glasses. Relatively high δD values (-50 to -20‰) are associated with subduction zone fluids (green swirls, arc, backarc; e.g., Shaw et al., 2008) and with enriched mantle sources such as ocean island basalts (including Amsterdam-St. Paul, Easter; see **Fig. 6**). Other submarine basalts, including the highest ³He/⁴He basalts from Loihi Seamount, have lower δD near -75‰ and may be sampling primordial mantle hydrogen (purple dots) that is dominantly derived from a deep mantle plume source. Very low δD values <-90‰ are found in some midocean ridge basalts derived from highly depleted upper mantle domains, sometimes present beneath intra-transform spreading centers. These ultra- depleted MORB glasses may carry a signature of multi-stage melting of their mantle source and isotopic fractionation associated with nominally anhydrous minerals in the residue (light blue dots). Mid-ocean ridge basalts are more commonly melts derived from larger mantle domains that appear to still sample some primordial hydrogen. [2 column width]